



CrossMark
click for updates

Cite this: *RSC Adv.*, 2016, 6, 9315

Received 28th November 2015
Accepted 14th January 2016

DOI: 10.1039/c5ra25320a

www.rsc.org/advances

Fuel cell anode catalyst performance can be stabilized with a molecularly rigid film of polymers of intrinsic microporosity (PIM)

Daping He,^a Yuanyang Rong,^a Mariolino Carta,^b Richard Malpass-Evans,^b Neil B. McKeown^b and Frank Marken^{*a}

There remains a major materials challenge in maintaining the performance of platinum (Pt) anode catalysts in fuel cells due to corrosion and blocking of active sites. Herein, we report a new materials strategy for improving anode catalyst stability based on a protective microporous coating with an inert and highly rigid (non-blocking) polymer of intrinsic microporosity (PIM-EA-TB). The “anti-corrosion” effect of the PIM-EA-TB coating is demonstrated with a commercial Pt catalyst (3–5 nm diameter, 40 wt% Pt on Vulcan-72) and for three important fuel cell anode reactions: (i) methanol oxidation, (ii) ethanol oxidation, and (iii) formic acid oxidation.

Fuel cells powered by oxidation of small organic molecules (such as methanol, ethanol, formic acid, *etc.*) can be highly efficient, environmentally friendly, convenient in terms of fuel storage and infrastructure, and relatively simple in terms of device manufacturing.^{1–4} A significant challenge remaining in the large-scale implementation of low temperature fuel cells (such as polymer-electrolyte or PEM fuel cells for cars) is the often rapid degradation of catalysts (depending on operational conditions) in both anode and cathode compartments due to catalyst migration, Ostwald ripening, carbon substrate corrosion, and loss of catalyst from the surface.^{5,6} These losses are often linked to short operational bursts or switching during power generation. This leads to the irreversible decay of fuel performance associated with additional costs of maintenance.^{1,7–9} Conditions during operational deterioration of catalysts can be simulated by accelerated degradation testing (ADT) based on repeated potential cycles.

Due to the insufficient activity of non-noble metal catalysts, the most commonly used fuel cell catalysts to date are 3–5 nm diameter Pt nanoparticles, which are supported on commercial carbon supports such as Vulcan-72.^{10,11} The well-known detrimental corrosion processes for Pt nanocatalysts include

electro-corrosion *via* Pt dissolution and colloidal mobility, aggregation, and poisoning by intermediates and corrosion products during small organic fuel molecule oxidation.^{12–14} A simple materials solution such as a protective coating is highly desirable.

Employing polymer functionalization to optimize the performance of commercial Pt/C catalysts and to design new nano-composite catalyst systems are both promising strategies for fuel cell catalyst development and engineering. Some advanced polymers, such as polyaniline (PANI)^{13,15–17} or PTFE/perfluorosulfonic acid (PFSA)^{18–20} have received special attention in fuel cell catalyst stabilization, because of their unique conductive and/or proton mobility properties. Interfacial Pt-catalyst engineering for example with pyridine-containing poly-benzimidazole on multi-walled carbon nanotubes has been reported to improve catalyst performance for methanol fuel cells.²¹ These materials lead locally to high electrical and proton conductivity and good chemical stability in acidic environments. However, due to poor rigidity these materials also strongly interact with catalyst surfaces. Challenges are still considerable in precisely controlling the thickness of these solid polymer over-layers, which also increase the resistance towards reaction species transport to the catalyst surface and so detrimentally affect catalytic activity. A polymer with more rigid molecularly pre-defined microporosity could be a better alternative. The rigid structure of the polymer can maintain a permanent microporosity, which facilitates the transportation of the reaction species whilst suppressing morphological changes.

Recently, the novel class of intrinsically microporous polymer (PIM) materials has been developed primarily for a range of applications in gas membrane technology.^{22–26} The structurally highly rigid PIM backbone achieves open packing to generate novel properties due to permanent microporosity. In our recent publications we have demonstrated benefits of PIM materials also in aqueous electrolyte media with potential applications emerging in electrochemical technology^{27,28} and in solution phase electrocatalysis.^{29–32} Particularly useful is a novel amine-containing PIM

^aDepartment of Chemistry, University of Bath, Claverton Down, Bath BA2 7AY, UK. E-mail: f.marken@bath.ac.uk

^bSchool of Chemistry, University of Edinburgh, David Brewster Road, Edinburgh, EH9 3FJ, UK

(PIM-EA-TB), synthesised *via* a polymerisation reaction involving the formation of Tröger's base with high molecular mass ($M_w > 70\,000\text{ g mol}^{-1}$) and high BET surface area ($1027\text{ m}^2\text{ g}^{-1}$). This PIM material was shown to be applicable as an effective protection agent against Pt/C catalysts corrosion in fuel cell cathodes³² (for oxygen reduction). In this report, it is demonstrated that the same methodology can be applied much more generally also for fuel cell anode catalysts in methanol, ethanol, or formic acid oxidation.

The rigid microporous PIM-EA-TB film is employed here as a coating to encapsulate the Pt/C catalysts (see Fig. 1a) whilst maintaining effective diffusion channels of 1–3 nm diameter²⁶ for water and reaction species. The coating is applied on top of the catalyst composite layer by casting of a PIM-EA-TB solution in chloroform. A layer of 10 μg PIM-EA-TB is applied to a 6 mm diameter glassy carbon electrode with underlying catalyst to give a film of approximately 40 nm average thickness (or lower when taking into account surface roughness of the catalyst layer). The TEM image of commercial Pt/C catalyst (40 wt% on Vulcan-72) in Fig. 1b shows a size range of 3 to 5 nm for Pt nanoparticles supported on carbon black. Fig. 1c and d show SEM images of Pt/C (c) and PIM@Pt/C (d) catalysts. The PIM-EA-TB membrane layer was found distributed over catalyst layer surface (appearing as “haze” in the SEM image), which suggests a successful modification of the PIM-EA-TB film on top of the Pt/C catalyst.

Data in Fig. 2a shows cyclic voltammetry responses for Pt/C (black) and for PIM@Pt/C (red) immersed in N_2 -saturated 0.1 M HClO_4 at room temperature. Both voltammetric responses are dominated by the classic platinum surface signals and essentially identical. That is, under these conditions there is no direct effect of the PIM-EA-TB surface layer on these signals. The rigid molecular structure prevents blocking of surface sites on the platinum. The electrochemically active surface area (ESA) for the catalyst can be calculated from

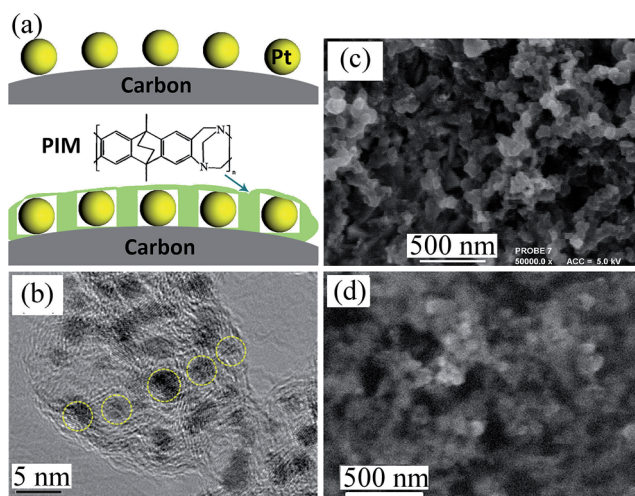


Fig. 1 (a) Schematic illustration of PIM-EA-TB rigidly encapsulating and protecting Pt/C catalyst without blocking the surface. (b) TEM image of Pt/C catalyst. SEM images for Pt/C (c) and PIM@Pt/C (d) on glassy carbon electrode substrate.

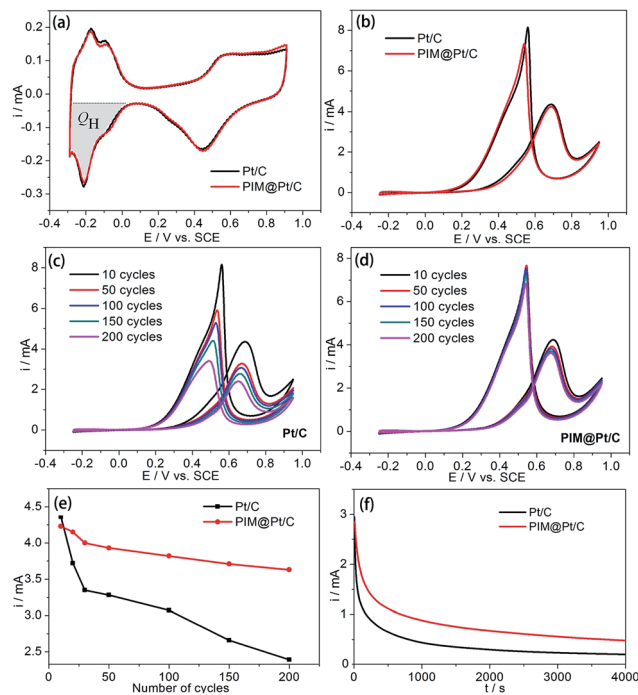


Fig. 2 (a) Cyclic voltammograms in N_2 -saturated 0.1 M HClO_4 (50 mV s^{-1}) and (b) cyclic voltammograms for methanol oxidation in 0.1 M HClO_4 + 1 M CH_3OH for Pt/C and for PIM@Pt/C. (c and d) Cyclic voltammograms for Pt/C (c) and for PIM@Pt/C (d) showing accelerated degradation testing from -0.25 to $+0.95\text{ V vs. SCE}$. (e) Plot of electrocatalytic oxidation peaks for Pt/C and for PIM@Pt/C for the forward peak current for ethanol electro-oxidation over 200 cycles. (f) Chronoamperometric curves of Pt/C and PIM@Pt/C at $+0.6\text{ V vs. SCE}$.

measuring the charge collected in the hydrogen adsorption/desorption region (see Q_H) and assuming $210\text{ }\mu\text{C cm}^{-2}$.³³ Values obtained in this way are $53.4\text{ m}^2\text{ g}^{-1}$ for Pt/C and $52.5\text{ m}^2\text{ g}^{-1}$ for PIM@Pt/C. This provides strong evidence that only few surface Pt atoms are inactivated by bonding to the amine functionality within the PIM-EA-TB, which is due to the highly rigid and conformationally locked structure of the polymer.

Methanol electro-oxidation (which is important in direct methanol fuel cells³⁴) was investigated in aqueous 0.1 M HClO_4 + 1 M CH_3OH as shown in Fig. 2b. The process is known to yield predominantly carbon dioxide. The Pt/C and PIM@Pt/C catalysts show very similar onset potential and peak currents for methanol electro-oxidation, at least initially. Then, the long-term electrocatalytic stability for PIM@Pt/C and commercial Pt/C were tested by repeating the cyclic voltammetry potential sweeps for 200 cycles (see Fig. 2c and d).

Whereas Pt/C catalyst (Fig. 2c) suffers significant degradation and decay in the catalytic current (due to the harsh accelerated degradation conditions), the PIM@Pt/C catalyst (see Fig. 2d) remains stable under these conditions. Fig. 2e shows the normalized forward oxidation peak current *versus* the number of potential cycle for both catalysts, which demonstrates that the decrease of the forward peak current of PIM@Pt/C is much slower compared to that for the commercial unprotected Pt/C catalyst. After 200 potential cycles, 88% of the initial forward oxidation peak current was maintained for

PIM@Pt/C as compared to only 48% for Pt/C. Additionally, chronoamperometry test measurements were performed in aqueous 1 M methanol + 0.1 M HClO₄ at the oxidation potential of 0.6 V vs. SCE (see Fig. 2f). After 4000 s, the current is 0.48 mA for PIM@Pt/C and only 0.21 mA for Pt/C – again indicative of enhanced catalyst stability during methanol oxidation. The results show significant benefits even at shorter times. This suggests that the polymer microporosity, in addition to enhancing durability due to corrosion protection, may help to maintain surface activity due to prevention of impurity adsorption and blocking.

Ethanol electro-oxidation (of interest for direct ethanol fuel cells³⁴) was investigated under similar conditions (see Fig. 3a–d). Products for the process include carbon dioxide and acetic acid. Measurements are reported for PIM@Pt/C and Pt/C in the aqueous 0.1 M HClO₄ + 1 M ethanol at room temperature.

Very similar cyclic voltammetry responses are obtained for ethanol electro-oxidation on both types of catalysts (Fig. 3a). For the accelerated durability testing, cyclic voltammetry potential scans were performed for 500 continuous cycles. Fig. 3b and c contrast the behaviour observed with/without the PIM-EA-TB film coating during durability testing. A significant decay in performance is seen only for the commercial Pt/C catalyst. Fig. 3d shows the forward oxidation peak current density as a function of cyclic voltammetry scan number and demonstrates that the forward oxidation peak current density of PIM@Pt/C catalyst reaches the maximum (3.9 mA) at the 100th cycle, and then remains relatively constant. The initial increase could be linked to some relaxation in the polymer film. In contrast, a slow but monotonous decrease in catalyst performance with the number of potential cycle is seen on the commercial Pt/C catalyst. This behaviour is usually attributed to surface poisoning by CO-like species as well as the dissolution loss of Pt from the surface. After 500 potential cycles, 98% of the

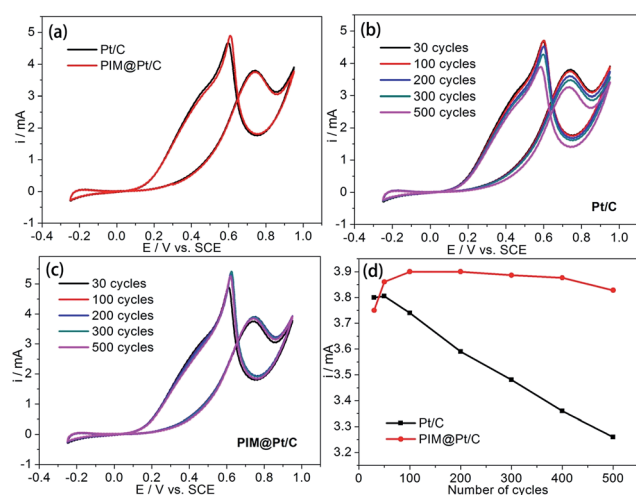


Fig. 3 (a) Cyclic voltammograms for ethanol oxidation recorded at room temperature in 0.1 M HClO₄ + 1 M CH₃CH₂OH (50 mV s⁻¹). (b and c) Cyclic voltammograms for Pt/C (c) and for PIM@Pt/C (d) for accelerated degradation testing from -0.25 to +0.95 V vs. SCE. (d) Plot of electrocatalytic peak currents of Pt/C and PIM@Pt/C referring to the forward peak current for ethanol electro-oxidation over 500 cycles.

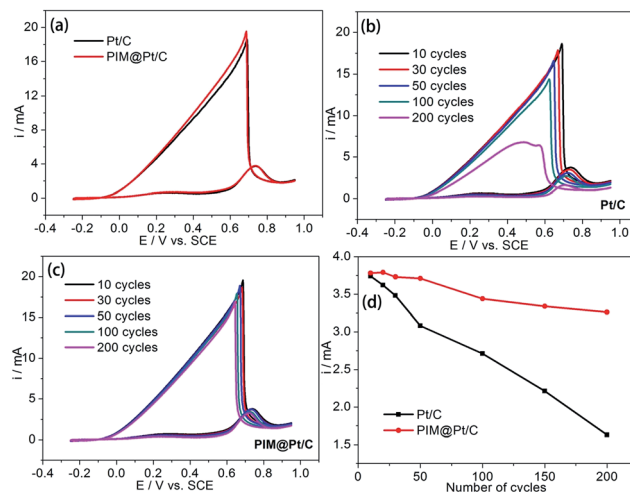


Fig. 4 (a) Cyclic voltammograms for formic acid oxidation at room temperature in a 0.1 M HClO₄ + 1 M HCOOH (50 mV s⁻¹). (b and c) Cyclic voltammograms for Pt/C (c) and for PIM@Pt/C (d) for accelerated degradation testing by potential cycling from -0.25 to +0.95 V vs. SCE. (d) Plot of oxidation peak currents for Pt/C and for PIM@Pt/C for the forward peak for formic acid electro-oxidation over 200 cycles.

initial forward oxidation peak current was still maintained for PIM@Pt/C, as compared to the decrease to 85% of initial activity for Pt/C.

Formic acid electro-oxidation (for direct formic acid fuel cells³⁵) activity was tested in aqueous 0.1 M HClO₄ + 1 M HCOOH (see Fig. 4a). The process is known to lead to carbon dioxide as the principle product. Initially, both the Pt/C and the PIM@Pt/C catalysts show very comparable activities for formic acid electro-oxidation. The accelerated degradation testing by cyclic voltammetry and monitoring electrocatalytic performance for PIM@Pt/C and for commercial Pt/C are shown in Fig. 4b and c. It can be seen that current peaks for commercial Pt/C catalyst (Fig. 4b) change significantly, while the equivalent experiments with PIM@Pt/C (Fig. 4c) demonstrate much greater robustness. The backward potential scan oxidation peak drops dramatically.

The result for the forward scan oxidation peak currents *versus* number of potential cycles for both Pt/C and PIM@Pt/C are shown in Fig. 4d. After 200 potential cycles, 85% of the initial forward oxidation peak current was still maintained for PIM@Pt/C, whereas only 43% activity remained for Pt/C. This again demonstrates enhanced durability during accelerated degradation testing when the PIM-EA-TB coating is applied to the catalyst.

Conclusions

A significant improvement in catalyst durability and performance (under accelerated degradation conditions) has been achieved by applying a PIM-EA-TB film as protective over-coating to commercial fuel cell anode catalyst materials. It is suggested that the molecularly rigid and microporous nature of the PIM-EA-TB material are crucial in (i) mechanically

stabilizing both carbon substrate and platinum nano-catalyst, (ii) preventing electrophoretic mobility, (iii) not directly interacting with the platinum nano-catalyst surface sites, whilst (iv) preventing larger adsorbates reaching the catalyst surface. Enhanced stability does not come at the cost of reduced performance as the flow of reagents and charges through the microporous PIM-EA-TB environment is sufficient for good catalysis. Materials properties at the molecular level are important for catalyst performance improvement for a range of potential fuel cell technologies (and beyond). We believe our methodology provides a new and general route to increase fuel cell anode catalyst performance and lifetime.

Experiment section

Chemical reagents

Commercial Pt/C (40 wt% on Vulcan-72) catalysts and Nafion (5 wt%) were obtained from Johnson Matthey and Dupont, respectively. Isopropanol, chloroform, and perchloric acid (70–72%), were purchased from Aldrich or Fisher Scientific and used without further purification. PIM-EA-TB was prepared following a literature recipe.³⁶ Solutions were prepared with filtered and deionized water of resistivity 18.2 MW cm from a Thermo Scientific water purification system (ELGA).

Instrumentation and procedures

Electrochemical measurements were performed with a μ Auto-lab III system in a conventional three electrode cell with KCl-saturated calomel (SCE) reference and platinum wire counter electrode. A Pine AFMSRCE electrode rotator was used for rotating disk electrode (RDE) experiments. Data obtained in stationary solution and with rotation were essentially identical and therefore only stationary experiments are reported here. Morphologies of the prepared catalysts were analyzed with a JEOL FESEM 6301F scanning electron microscopy (SEM) and a JEOL 2010 high-resolution transmission electron microscope (HRTEM).

Procedures for electrode preparation

2 mg of Pt/C catalyst and 100 μ L of 5 wt% Nafion solution were dispersed in 1 mL of isopropanol, followed by a sonication for at least 15 min to form a homogeneous catalyst ink. A volume of 8 μ L of the ink was loaded onto a glassy carbon (GC) disk electrode with a diameter of 6 mm. The catalyst layer was allowed to dry under ambient conditions before a CV measurement. Polymer with intrinsic microporosity coating Pt/C (PIM@Pt/C) was conducted as follow: a solution of 1 mg cm⁻³ PIM-EA-TB was prepared in chloroform and 10 μ L was applied directly by coating the Pt/C catalyst layer followed by drying under ambient conditions.

Acknowledgements

D. H. thanks the Royal Society for a Newton International Fellow. F. M. and N. M. thank the Leverhulme Trust for support (RPG-2014-308). F. M. thanks Dr Robert Potter from Johnson-Matthey for support with catalyst materials and for helpful discussion.

References

- H. Liu, C. Song, L. Zhang, J. Zhang, H. Wang and P. Wilkinson, *J. Power Sources*, 2006, **155**, 95.
- S. K. Kamarudin, F. Achmad and W. R. W. Daud, *Int. J. Hydrogen Energy*, 2009, **34**, 6902.
- M. Z. F. Kamarudin, S. K. Kamarudin, M. S. Masdar and W. R. W. Daud, *Int. J. Hydrogen Energy*, 2013, **38**, 9438.
- X. Yu and P. G. Pickup, *J. Power Sources*, 2008, **182**, 124.
- J. Park, H. Oh, T. Ha, Y. I. Lee and K. Min, *Appl. Energy*, 2015, **155**, 866.
- L. Li, L. P. Hu, J. Li and Z. D. Wei, *Nano Res.*, 2015, **8**, 418.
- X. Zhao, M. Yin, L. Ma, L. Liang, C. P. Liu, J. H. Liao, T. H. Lu and W. Xing, *Energy Environ. Sci.*, 2011, **4**, 2736.
- F. Vigier, C. Coutanceau, A. Perrard, E. M. Belgsir and C. Lamy, *J. Appl. Electrochem.*, 2004, **34**, 439.
- C. Rice, S. Ha, R. I. Masel and A. Wieckowski, *J. Power Sources*, 2003, **115**, 229.
- N. C. Cheng, M. N. Banis, J. Liu, A. Riese, X. Li, R. Y. Li, S. Y. Ye, S. Knights and X. L. Sun, *Adv. Mater.*, 2015, **27**, 277.
- N. C. Cheng, M. N. Banis, J. Liu, A. Riese, S. C. Mu, R. Y. Li, T. K. Sham and X. L. Sun, *Energy Environ. Sci.*, 2015, **8**, 1450.
- E. G. Ciapina, S. F. Santos and E. R. Gonzalez, *J. Electroanal. Chem.*, 2010, **644**, 132; S. Chen, Z. Wei, X. Qi, L. Dong, Y. Guo, L. Wan, Z. Shao and L. Li, *J. Am. Chem. Soc.*, 2012, **134**, 13252.
- M. W. Breiter, *J. Electroanal. Chem. Interfacial Electrochem.*, 1967, **15**, 221.
- M. Zhiani, B. Rezaei and J. Jalili, *Int. J. Hydrogen Energy*, 2010, **35**, 9298.
- D. P. He, C. Zeng, C. Xu, N. C. Cheng, H. G. Li, S. C. Mu and M. Pan, *Langmuir*, 2011, **27**, 5582.
- M. Zhiani, B. Rezaei and J. Jalili, *Int. J. Hydrogen Energy*, 2010, **35**, 9298.
- D. P. He, S. C. Mu and M. Pan, *Carbon*, 2011, **49**, 82.
- D. P. He, K. Cheng, H. G. Li, T. Peng, F. Xu, S. C. Mu and M. Pan, *Langmuir*, 2012, **28**, 3979.
- Z. Q. Tian, S. P. Jiang, Z. Liu and L. Li, *Electrochem. Commun.*, 2007, **9**, 1613.
- N. B. McKeown and P. M. Budd, *Macromolecules*, 2010, **43**, 5163.
- T. Fujigaya, M. Okamoto, K. Matsumoto, K. Kaneko and N. Nakashima, *ChemCatChem*, 2013, **5**, 1701.
- N. B. McKeown, B. Gahnem, K. J. Msayib, P. M. Budd, C. E. Tattershall, K. Mahmood, S. Tan, D. Book, H. W. Langmi and A. Walton, *Angew. Chem., Int. Ed.*, 2006, **45**, 1804.
- C. G. Bezzu, M. Carta, A. Tonkins, J. C. Jansen, P. Bernardo, F. Bazzarelli and N. B. McKeown, *Adv. Mater.*, 2012, **24**, 5930.
- S. V. Adymkanov, Y. P. Yampolskii, A. M. Polyakov, P. M. Budd, K. J. Reynolds, N. B. McKeown and K. J. Msayib, *Polym. Sci.*, 2008, **50**, 444.
- P. M. Budd, N. B. McKeown, B. S. Ghanem, K. J. Msayib, D. Fritsch, L. Starannikova, N. Belov, O. Sanfirova, Y. P. Yampolskii and V. Shantarovich, *J. Membr. Sci.*, 2008, **325**, 851.

- 26 E. Madrid, Y. Rong, M. Carta, N. B. McKeown, R. M. Evans, G. A. Attard, T. J. Clarke, S. H. Taylor, Y. Long and F. Marken, *Angew. Chem.*, 2014, **40**, 10927.
- 27 E. Madrid, P. Cottis, Y. Rong, A. T. Rogers, J. M. Stone, R. Malpass-Evans, M. Carta, N. B. McKeown and F. Marken, *J. Mater. Chem. A*, 2015, **3**, 15849.
- 28 F. J. Xia, M. Pan, S. C. Mu, R. Malpass-Evans, M. Carta, N. B. McKeown, G. A. Attard, A. Brew, D. J. Morgan and F. Marken, *Electrochim. Acta*, 2014, **46**, 26.
- 29 Y. Y. Rong, R. M. Evans, M. Carta, N. B. McKeown, G. A. Attard and F. Marken, *Electroanalysis*, 2014, **26**, 904.
- 30 Y. Y. Rong, R. M. Evans, M. Carta, N. B. McKeown, G. A. Attard and F. Marken, *Electrochem. Commun.*, 2014, **46**, 26.
- 31 D. P. He, Y. Y. Rong, Z. K. Kou, S. C. Mu, T. Peng, R. Malpass-Evans, M. Carta, N. B. McKeown and F. Marken, *Electrochem. Commun.*, 2015, **59**, 72.
- 32 C. E. Hotchen, G. A. Attard, S. D. Bull and F. Marken, *Electrochim. Acta*, 2014, **137**, 484.
- 33 S. Wasmus and A. Kuver, *J. Electroanal. Chem.*, 1999, **461**, 14.
- 34 Z. Y. Zhou, Z. Z. Huang, D. J. Chen, Q. Wang, N. Tian and S. G. Sun, *Angew. Chem., Int. Ed.*, 2010, **49**, 411.
- 35 X. W. Yu and P. G. Pickup, *J. Power Sources*, 2008, **182**, 124.
- 36 M. Carta, R. Malpass-Evans, M. Croad, Y. Rogan, J. C. Jansen, P. Bernardo, F. Bazzarelli and N. B. McKeown, *Science*, 2013, **339**, 303.